J. Cent. South Univ. (2015) 22: 2665−2680
DOI: 10.1007/s11771-015-2797-y

Springer

Formation mechanisms and distribution of high quality reservoirs in deep strata in Palaeogene in northern steep slope zone of Bonan sag, Jiyang depression, China

MA Ben-ben(马奔奔), CAO Ying-chang(操应长), JIA Yan-cong(贾艳聪), WANG Yan-zhong(王艳忠)

School of Geosciences, China University of Petroleum, Qingdao 266580, China

Abstract: Petrographic analysis combined with various techniques, such as thin section identification, petro-physical property testing, mercury penetration, oil testing results, was used to assess basic reservoir characteristics of deep strata in Palaeogene in the northern steep slope zone of the Bonan sag, China. The formation mechanisms of high quality reservoirs in deep strata were discussed according to evolution characteristics of paleopressures and paleofluids in geological period. The deep reservoirs have poor physical properties and mainly develop extra-low porosity, extra-low and ultra-low permeability reservoirs. Reservoir spaces mainly consist of secondary pores and overpressure fractures. Early overpressure, early hydrocarbon filling and dissolution by early organic acids are the major formation mechanisms of high quality reservoirs. The conglomerate in inner fan which had a poor primary physical property mainly experienced strong compaction and calcareous matrix recrystallization. The physical properties of the inner fan were poor with weak dissolution because of poor mobility of fluid. The reservoirs mainly are type IV reservoirs and the distribution extends with the burial depth. The braided channel reservoirs in the middle fan had relative good primary physical properties and strong ability to resist compaction which favored the preservation of primary pores. Large amounts of the secondary porosities were created due to dissolution by early organic acids. A series of micro-fractures generated by early overpressures would be important migration pathways for hydrocarbon and organic acids. Furthermore, early overpressures had retarded maturation of organic matters and organic acids which had flowed into reservoirs already and could keep in acid environment for a long time. This process would contribute significantly to reinforcing the dissolution and enhancing the reservoir quality. The braided channel reservoirs were charged with high oil saturation preferentially by early hydrocarbon filling which could inhibit later cementation. Therefore, the braided channel reservoirs develop a great quantity of reservoir spaces with type I, type II and type III reservoirs in the majority in the deep strata. With the burial depth, distributions of type I and type II reservoirs are narrowed and distribution of type III reservoirs decreases first and then extends. The reservoirs both in outer fan and in interdistributary of the middle fan have extremely poor physical properties because of extensive carbonate cementation. The type of the reservoirs mainly is type IV.

Key words: deep strata; high quality reservoirs; formation mechanism; Palaeogene; Bonan sag

1 Introduction

Petroleum exploration in deep reservoirs, which refers to those at burial depth more than 3 km, deserves more specialized attention worldwide [1−6]. As petroleum exploration technology advances, the relative high quality reservoirs could be developed in the context of general low porosity and low permeability, and these sweet spots in deep reservoirs are characterized by better rounded, good sorting and small amounts of authigenic cements. Great heterogeneity of deep reservoirs is commonly demonstrated because of complex evolution of diagenesis and physical property. Consequently, identifying genetic mechanism and distribution of high quality reservoirs can provide guidance theoretically on petroleum exploration in deep strata.

With a relatively mature exploration on shallow strata in the northern steep slope zone of the Bonan sag, China, the upper part of the fourth member of the Shahejie formation (Es4s) in Palaeogene is identified as the main areas of current deep exploration interest and enormous potentials for petroleum exploration on Es4s are visible with oil testing results [7]. However, deep reservoirs had undergone multi-stage of cementation, dissolution, hydrocarbon-filling and complex metasomatism, as well as overpressures in the burial history [7−10]. As a result, physical properties of the reservoirs went through complicated evolutionary process. The aim of the present work is to have a detailed description of the

Foundation item: Project(41102058) supported by the National Natural Science Foundation of China; Project(2011ZX05006-003) supported by National Oil & Gas Major Project of China; Project(U1262203) supported by Key Program for National Natural Science Foundation of China; Project(LW140101A) supported by Excellent Doctoral Dissertation Program of China University of Petroleum
Received date: 2014−05−04; **Accepted date:** 2015−01−10
Corresponding author: CAO Ying-chang, PhD; E-mail: cyc8391680@163.com

characteristics of deep reservoirs and to identify formation mechanisms and distribution of high quality reservoirs in palaeogene in the northern steep slope zone of the Bonan sag, by means of petrographic analysis combined with thin section identification, petro-physical property testing, mercury penetration and oil testing results.

2 Regional geological setting

The Bonan sag, located in the northern part of the Jiyang depression, China, is a NE-strike, fault-subsidence lacustrine basin and contains a steep slope zone in the north and a gentle slope zone in the south. The sag is bounded to the east by the Guxi fault, to the west by the Yidong fault and to the south by the slope of the Chenjiazhuang salient. In the north, the Chengdong salient borders the sag, and this contact is marked by the Chengnan fault [11]. The Bonan sag covers an area of 600 km^2. The Palaeogene mainly consists of the Kongdian formation, Shahejie formation and Dongying formation from bottom to top in the Bonan sag. The Shahejia formation can be divided into four members, namely the fourth member (Es4), the third member (Es3), the second member (Es2), and the first member (Es1) from bottom up. During the deposition of Es4s, nearshore subaqueous fans were developed and large-scales of sandy conglomerate bodies with a maximum thickness of 800 m were deposited on the downthrown side of the Chennan fault in the northern steep slope zone of the Bonan sag (Fig. 1). These sandy conglomerate bodies are adjacent to lacustrine source rocks and thereby they possess great potentials for exploration with excellent geologic conditions for hydrocarbon accumulation. So far, exploration for sandy conglomerate bodies has made major breakthroughs in the northern steep slope of the Bonan sag. Wells Yigeng103, Yi104-1 and Yi109-1 have obtained industrial oil flows with a high level of productivity [11]. The nearshore subaqueous fan can be sub-divided into inner fan, middle fan and outer fan subfacies according to depositional characteristics and hydrodynamic condition (Fig. 2). Lithologies of the inner fan subfacies are mainly composed of poor sorted, matrix-supported conglomerates with angular and subangular gravels (Fig. 2). Matrix-supported conglomerates with a great thickness barely have apparent variation vertically in the inner fan, where almost no lacustrine mudstones are observed because of scouring erosion. The middle fan subfacies could be sub-divided into braided channel and interdistributary microfacies. Lithologies of the braided channel microfacies are principally characterized by pebbly sandstones and medium-coarse sandstones (Fig. 2). They are moderately-well sorted with low matrix contents and high level of textural maturity. Sedimentary structures are primarily characterized by normal graded bedding, scour surface as well as contemporaneous deformation structure in the braided channel microfacies. Lithologies of the interdistributary microfacies are mainly composed of typical turbidites featured by thin layers and fine grained (Fig. 2). Normal lacustrine mudstones could be developed among multi-periods of normal graded sandy conglomerate bodies in the middle fan subfacies. Lithologies of the

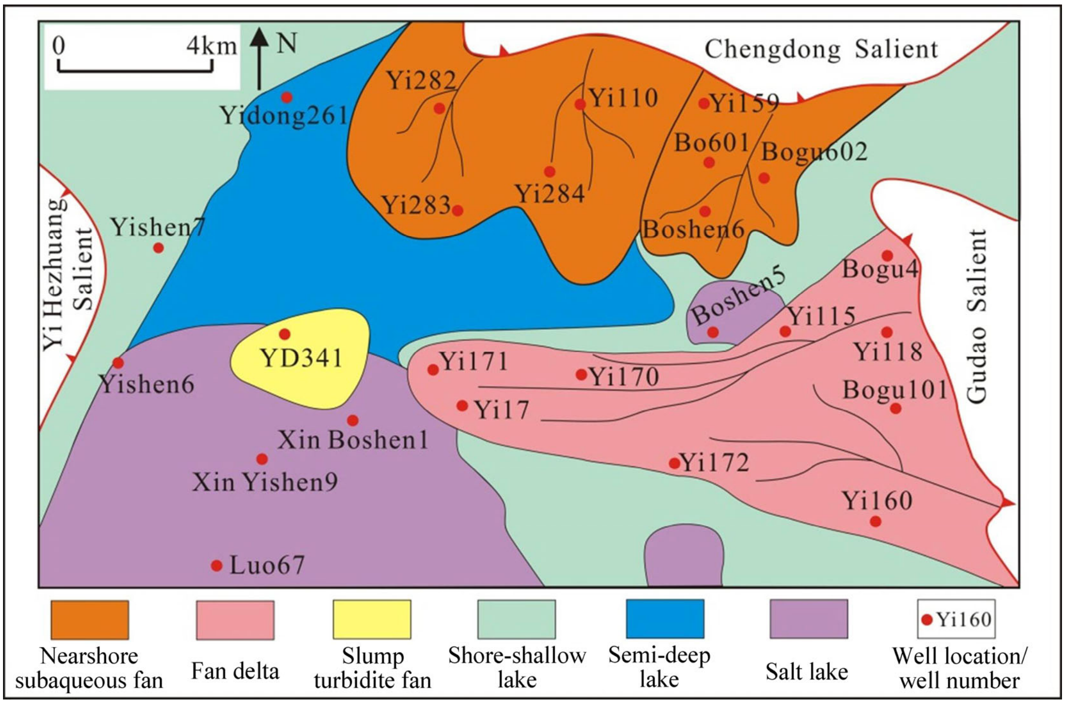

Fig. 1 Sedimentary facies of Es4s in Bonan sag (According to Ref. [12], modified)

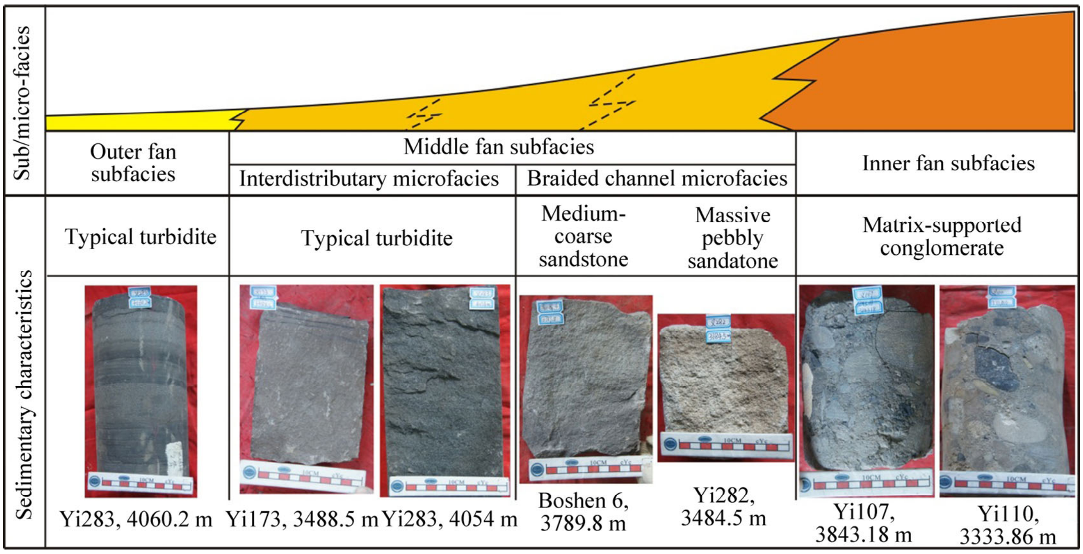

Fig. 2 Sedimentary characteristics of different sub/micro-facies in nearshore subaqueous fan

outer fan microfacies consist of dark gray mudstones intercalated by thin sandstones and pebbly sandstones (Fig. 2).

3 Reservoir characteristics

3.1 Petrography

Reservoir lithologies of the nearshore subaqueous fan of Es4s in the northern steep slope zone of the Bonan sag, China, are characterized by conglomerates, pebbly sandstones, sandstones and dark gray mudstones. The conglomerates are matrix-supported with major calcareous matrix as well as minor shaly one. Gravels which are angular-subrounded are mainly composed of limestone and granite-gneiss. Point counting data show that clastic grains are composed of quartz with an average mass fraction of 36.4%, feldspar 33.2% and rock fragments 30.4% ($Q_{36.4}F_{33.2}R_{30.4}$), which indicates that Es4s sandstones are lithic arkose and feldspathic litharenite [13], as shown in Fig. 3. Unstable lithic grains are dominated by metamorphic and rare sedimentary or volcanic rock fragments. Matrix content ranges from 0.5% to 40% with an average of 8.3%. Cement content ranges from 0.5% to 35% with an average of 8.1%. The reservoirs contain carbonate cement as the most abundant minerals, with quartz overgrowths present in lesser amounts. Grains are poorly sorted as shown by sorting coefficient ranging from 1.44 to 3.44 with an average of 1.88. Generally, the textural maturity and compositional maturity is quite low in sandy conglomerate reservoirs of Es4s in the northern steep slope zone of the Bonan sag.

3.2 Reservoir space

More than 210 thin sections and cores from 16 boreholes of sandy conglomerate samples in the nearshore subaqueous fan of Es4s in the northern steep slope zone of the Bonan sag, are selected for determining the features of reservoir space. Secondary pores and fractures are identified as the two major types of the reservoir space in deep reservoirs. The secondary pores mainly include the dissolution pores of feldspars and rock fragments (70.3%) (Figs. 4(a) and (b)), as well as a small quantity of the dissolution pores of carbonate cement (12.5%) (Fig. 4(c)). A certain amount of primary pores (15.2%) are observed as well (Fig. 4(d)). Overpressure fractures are the main type of fractures in deep reservoirs. They can either bypass grains or break them up into small pieces, and show poor regularity and directionality (Figs. 4(e)−(i)). Complex reservoir spaces (Fig. 4(f)) can be formed by secondary pores and fractures because of their genetic correlation. Secondary pores can also be found under the circumstances where overpressure fractures are developed because overpressure fractures and later acid fluids are able to enter into reservoirs and thereby dissolution pores are easily formed. Some fractures are filled with the later carbonate cements (Figs. 4(g)−(i)).

3.3 Reservoir physical properties

Physical properties of the sandy conglomerate reservoirs are poor with a burial depth of 3000−4500 m in the nearshore subaqueous fan of Es4s in the northern steep slope zone of the Bonan sag. The porosities of the studied samples are extra-low, ranging from 1.3% to 17.6% with an average of 7.5%. The permeability shows a wide range from <0.01 to 130 mD and samples with ultra-low permeability and extra-low permeability are in the majority (Fig. 5). Porosity and permeability show a branch-like correlation (Fig. 5(a)). Most samples with lower porosities have higher permeabilities due to the

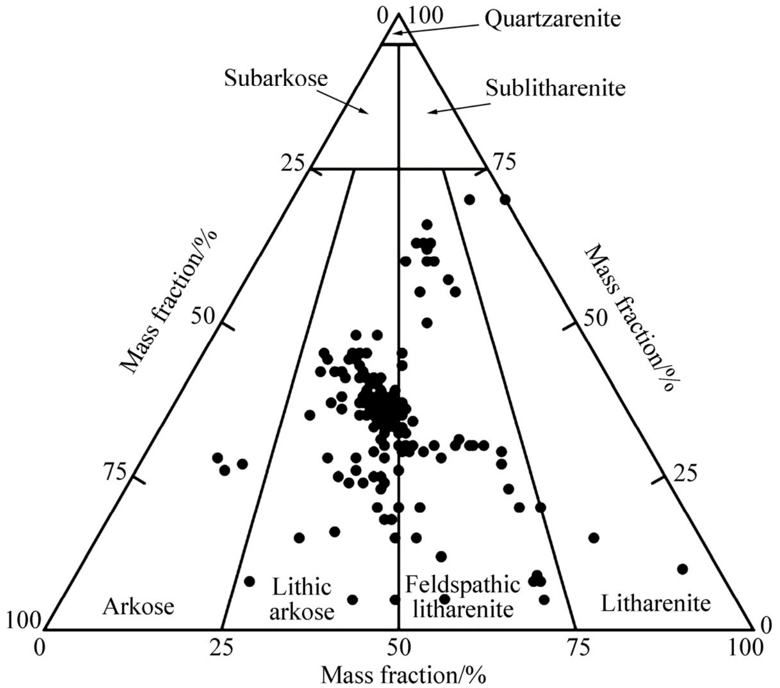

Fig. 3 Ternary diagram showing various types of sandstones identified in Es4s reservoirs

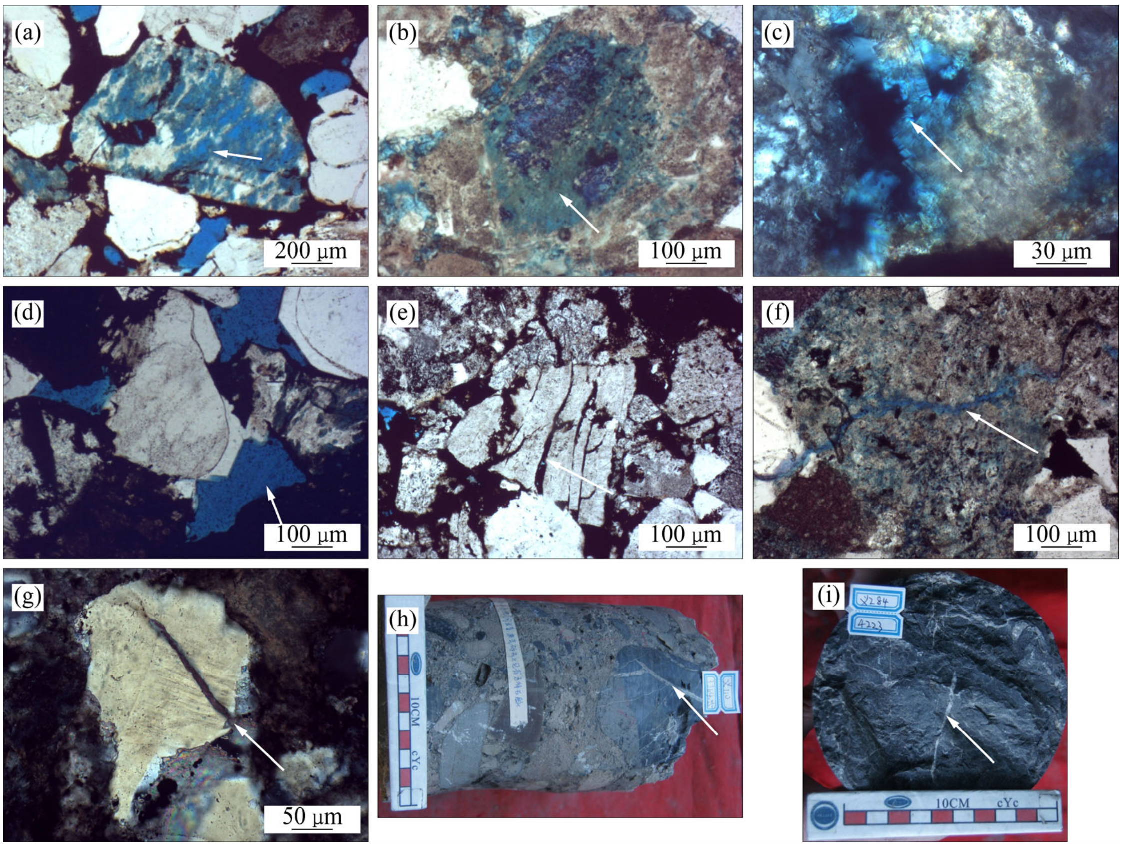

Fig. 4 Reservoir space in deep strata of Es4s in northern steep slope zone of Bonan sag: (a) Dissolution pores of feldspars, well Yi173, 4115.6 m, plane-polarized light; (b) Dissolution pores of feldspars filled by ferrocalcite, well Yi110, 3365.5 m, plane-polarized light; (c) Dissolution pores of carbonate cement, well Yi282, 3597.6 m, orthogonal polarized light; (d) Primary pores preserved by oil filling, well Yi173, 4115.2 m, plane-polarized light; (e) Overpressure fractures filled with oil, well Yi283, 3955.8 m, plane-polarized light; (f) Overpressure fractures, well Yi110, 3361.77 m, plane-polarized light; (g) Grain fractures filled with carbonate cements, well Yi285, 3972.1 m; (h) Grain fractures filled with carbonate cements from core observation, well Yi110, 3364.95 m; (i) Grain fractures filled with carbonate cements from core observation, well Yi284, 4223 m

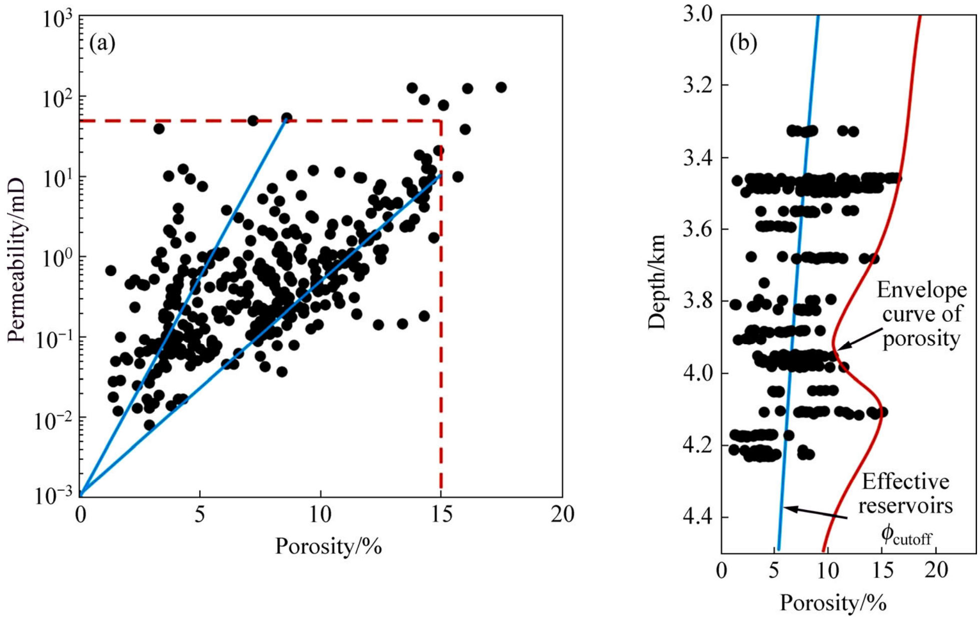

Fig. 5 Reservoir properties in deep strata of Es4s in northern steep slope zone of Bonan sag: (a) A plot of porosity versus permeability; (b) Relationship between porosity and burial depth (A total of 403 measured data of properties were from 16 wells. Porosity cutoff (ϕ_{cutoff}) of reservoir was calculated by formation test method using plenty of measured properties, logging interpretation properties and oil testing results, ϕ_{cutoff}=−9.1ln$H$+82.01, R^2=0.84 (φ_{cutoff}−Porosity cutoff; H−depth [14]); Data were from Hekou oil production plant in Shengli Oilfield)

presence of overpressure fracures which result in high permeability in deep strata. Progressive burial results in increasing compaction and porosity loss, and most reservoirs whose porosity is below the porosity cutoff of effective reservoirs become invalid while the rest whose porosity is above the cutoffs become high quality ones in moderately to deeply burial reservoirs (Fig. 5(b)).

4 Formation mechanism of high quality reservoirs

4.1 Early overpressure

Several methods can be used to restore paleopressures through fluid inclusion [15−17]. Using the homogenization temperature and the measured salinity of fluid inclusions, a relatively simple function was established by which the homogenization temperature could be related to the temperature and pressure of inclusion formation and the composition of the trapped fluid [17]:

$$p=A_1+A_2T \tag{1}$$

$$A_1=6.100\times10^{-3}+(2.385\times10^{-1}-a_1)T_h-(2.855\times10^{-3}+a_2)T_h^2-(a_3T_h+a_4T_h^2)m \tag{2}$$

$$A_2=a_1+a_2T_h+9.888\times10^{-6}T_h^2+(a_3+a_4T_h)m \tag{3}$$

where m=1000 W/[M×(100− w)] is molality; M is molar mass of NaCl; w is fluid inclusion salinity; T_h is homogenization temperature of fluid inclusion; p is the pressure; T is capture temperature of fluid inclusion and can be calibrated by T_h calibration curves of saline water inclusions [18]. In a NaCl−H_2O system, a_1=2.873×10^1, a_2= −6.477×10^{-2}, a_3=−2.009×10^{-1}, a_4=3.186×10^{-3}.

Therefore, the paleopressures could be reestablished in accordance with this method. The formation time for paleopressure is concluded from T_h of fluid inclusion in conjunction with the burial history (Table 1).

Paleopressure coefficients indicate that there were two peaks of formation pressure in the geological time (Fig. 6). The paleopressures were increasing quickly due to the disequilibrium compaction in the early rapid deposition, and reached its first peak with a pressure coefficient of 1.71, approximately 32.5 Ma ago. After 32.5 Ma, the paleopressures were reducing rapidly as a result of regional tectonic uplift and reached the minimum, about 24.6 Ma ago. The formation temperature went up quickly with strata subsiding once again, and source rocks of Es4s and Es3x [7−9] entered into thermal mature stage with the rising temperature. Eventually, the paleopressures increased again due to the hydrocarbon generation and reached its second peak with the pressure coefficient of 2.21 (Fig. 6). Evidently, pressure coefficient of the latter stage was much higher than that of the former stage. It illustrated that the latter overpressures induced by the hydrocarbon generation had exerted more important influence on reservoirs than the former one duo to the disequilibrium compaction.

Previous studies on overpressure generating mechanisms demonstrated that abnormal overpressure was generated by disequilibrium compaction in the early rapid deposition [19−21]. Three mechanisms about

Table 1 Paleo-pressures results reestablished by homogenization temperature and measured salinity of fluid inclusions

Well	Strata	Depth/m	Host mineral	Type	T_h/°C	Salinity/%	m/(mol·kg^{-1})	T/°C	A_1	A_2	p/MPa	Age/Ma	Paleo-depth/m	Paleo-hydrostatic pressure/MPa	Pressure coefficient
Boshen5	Es4s	5136	Quartz overgrowth	Salt-water	102.4	2.06	0.36	113.92	−2273	22.2	26.14	40	2000	19.6	1.33
Boshen5	Es4s	5136	Quartz overgrowth	Salt-water	100.8	5.25	0.95	112.05	−2254	22.4	25.74	41	1900	18.62	1.38
Yi120	Es4s	3038.2	Quartz overgrowth	Salt-water	104.2	0.53	0.09	116.02	−2298	22.1	26.63	35	1850	18.13	1.47
Yi120	Es4s	3038.2	Quartz overgrowth	Salt-water	102.9	1.90	0.33	114.51	−2281	22.2	26.29	37	1800	17.64	1.49
Yi129	Es4s	2213.9	Quartz overgrowth	Salt-water	128	10.49	2.00	143.81	−2686	21.0	33.68	8	2100	20.58	1.64
Yi129	Es4s	2213.9	Quartz overgrowth	Salt-water	129.1	3.85	0.68	145.10	−2665	20.7	33.53	8	2100	20.58	1.63
Yi129	Es4s	2213.9	Quartz overgrowth	Salt-water	98	22.66	5.01	108.78	−2252	23.0	25.37	9	2000	19.6	1.29
Yi129	Es4s	2243.5	Quartz overgrowth	Salt-water	135.7	7.15	1.32	152.81	−2768	20.4	35.39	8	2100	20.58	1.72
Yi129	Es4s	2243.5	Quartz overgrowth	Salt-water	133.6	6.72	1.23	150.35	−2738	20.5	34.84	8	2100	20.58	1.69
Yi129	Es4s	2243.5	Quartz overgrowth	Salt-water	134.8	6.43	1.18	151.76	−2752	20.4	35.12	8	2100	20.58	1.71
Yi129	Es4s	2396.7	Quartz overgrowth	Salt-water	110.8	1.05	0.18	123.73	−2400	21.7	28.54	14	1500	14.7	1.94
Yi129	Es4s	2396.7	Quartz overgrowth	Salt-water	119.9	4.32	0.77	134.36	−2543	21.2	31.17	14	1500	14.7	2.12
Yi129	Es4s	2396.7	Quartz overgrowth	Salt-water	124.9	5.25	0.95	140.20	−2616	21.0	32.54	14	1500	14.7	2.21
Yi129	Es4s	2396.7	Quartz overgrowth	Salt-water	122.6	4.01	0.71	137.51	−2579	21.1	31.87	14	1500	14.7	2.17
Yi160	Es4s	3128.5	Quartz overgrowth	Salt-water	104.6	15.04	3.03	116.49	−2345	22.5	27.21	27	2100	20.58	1.32
Yi160	Es4s	3128.5	Quartz overgrowth	Salt-water	81	1.39	0.24	88.93	−1903	23.6	19.28	34	1300	12.74	1.51
Yi160	Es4s	3129.3	Quartz overgrowth	Salt-water	141.8	15.14	3.05	159.93	−2904	20.5	37.64	2	3100	30.38	1.24
Yi160	Es4s	3130.7	Quartz overgrowth	Salt-water	115.7	19.95	4.26	129.45	−2550	22.1	30.84	6	2500	24.5	1.26
Yi172	Es4s	3955.1	Quartz overgrowth	Salt-water	127	21.42	4.66	142.65	−2740	21.6	34.27	9.5	2920	28.616	1.20
Yi172	Es4s	3955.1	Quartz overgrowth	Salt-water	120	18.87	3.98	134.47	−2614	21.8	32.04	13	2400	23.52	1.36
Yi172	Es4s	4079.48	Quartz overgrowth	Salt-water	103.5	12.88	2.53	115.21	−2319	22.5	26.79	30	1800	17.64	1.52
Yi173	Es4s	4115.2	Quartz overgrowth	Salt-water	140.85	14.20	2.83	158.82	−2883	20.5	37.30	9	3200	31.36	1.19
Yi173	Es4s	4115.2	Quartz overgrowth	Salt-water	139.2	21.35	4.64	156.89	−2923	21.0	37.66	9.4	3200	31.36	1.20
Yi173	Es4s	4115.2	Quartz overgrowth	Salt-water	125.8	18.87	3.98	141.25	−2704	21.5	33.71	12	2200	21.56	1.56
Yi173	Es4s	4115.2	Quartz overgrowth	Salt-water	98.7	7.99	1.48	109.60	−2226	22.6	25.16	32.6	1500	14.7	1.71
Yi173	Es4s	4115.6	Quartz overgrowth	Salt-water	122.9	23.56	5.27	137.86	−2690	21.9	33.25	12	2200	21.56	1.54
Yi173	Es4s	4115.6	Quartz overgrowth	Salt-water	132	21.20	4.60	148.49	−2815	21.4	35.66	13	2400	23.52	1.52
Yi173	Es4s	4115.6	Quartz overgrowth	Salt-water	132.5	15.55	3.15	149.07	−2780	21.0	35.27	13	2400	23.52	1.50
Yi283	Es4s	4056.4	Quartz overgrowth	Salt-water	120.5	15.20	3.04	135.06	−2601	21.6	31.94	22	2000	19.6	1.63
Yi283	Es4s	4184.3	Quartz overgrowth	Salt-water	130.6	14.65	2.92	146.85	−2747	21.1	34.68	20	2100	20.58	1.69

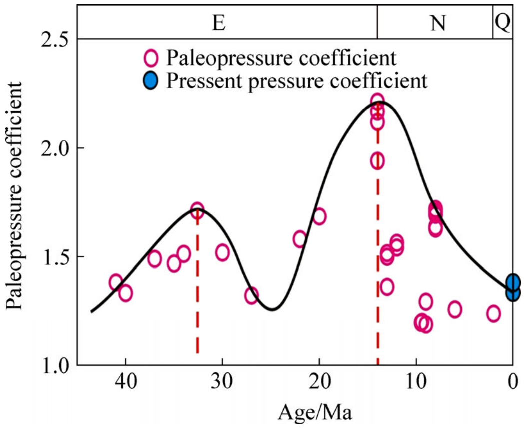

Fig. 6 Paleopressure coefficient evolution of Es4s in Bonan sag

porosity preservation by early overpressures have been proposed. Firstly, porosity that would otherwise be lost to compaction is held open by early overpressures in a low vertical effective stress regime, resulting in anomalously porous reservoirs [22−23]. Secondly, early overpressures have been suggested to limit or prevent significant quartz cementation by inhibiting intergranular pressure solution [21, 24]. Thirdly, early overpressures allow the potential development of secondary porosity [25].

A plot of present pressure-coefficient versus depth profile (Fig. 7) of sandy conglomerates in Es4s in the northern steep slope zone of the Bonan sag shows that the overpressures are generated at burial depth of 2000 m in a relatively early period. A trend of increasing overpressure with an increase of burial depth has been noted. The present pressure distribution is consistent with the restored results of paleopressures. Overpressures

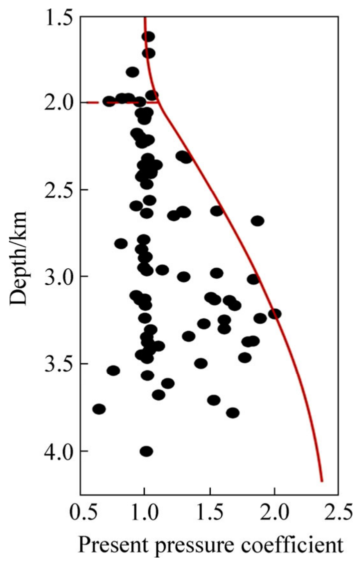

Fig. 7 A plot of present pressure coefficient versus depth profile of sandy conglomerates in Es4s in northern steep slope zone of Bonan sag (Measured stratigraphic pressures for a total of 84 samples were collected at different depths from 24 wells)

in the early period contribute to the maintenance of high primary porosities in a low vertical effective stress regime. Previous studies showed that overpressures induced in the early rapidly-deposited period were formed as box-like overpressure compartments by the regional caprocks made of lacustrine mudstones in Es4s and Es3x [7]. A series of micro-fractures could be formed when formation pressure exceeds fracture pressure during formation pressure accumulation [26]. The developed zones of overpressure micro-fractures coincide with the present overpressure zones (Figs. 4(e)−(i)).

Based on the episodic accumulation theory [27], these micro-fractures are defined as the important migration pathways for hydrocarbon and organic acid fluids. They will be resealed by reduced formation pressures after energy is released and are opened up the second time due to the hydrocarbon generation in the later period.

4.2 Early hydrocarbon filling

Previous studies have revealed two episodes of hydrocarbon filling in the sandy conglomerate reservoirs of Es4s in the northern steep slope zone of the Bonan sag [28−29].

The early stage of oil inclusions has green fluorescence color and the homogenization temperature (T_h) ranges from 85 °C to 110 °C. T_h for salt-water inclusions in the same period is 110−130 °C and their salinity is 1%−6%. In contrast, the later one of oil inclusions has blue−white fluorescence color and T_h ranges from 110 °C to 130 °C. T_h for salt-water inclusions in the same period is 130−150 °C and their salinity is 14%−22% [28]. Therefore, according to T_h for salt-water inclusions in these two periods and in conjunction with the burial history, the early hydrocarbon filling took place approximately 28.8−24.6 Ma ago; while the later one occurred 10−6 Ma ago. In spite of the limited amounts of hydrocarbon generated in the early period, effective hydrocarbon filling still occurred since the sandy conglomerate reservoirs are close to the center of hydrocarbon generating sag. Early overpressures were released during 32.5−24.6 Ma ago and the paleopressure coefficient dropped to 1.25, about 24.6 Ma ago (Fig. 6). Therefore, the early hydrocarbon filling which was generated approximately 28.8−24.6 Ma ago had hardly been inhibited by early overpressures.

Early hydrocarbon filling has been identified as an important factor for reservoirs conservation. On one hand, early hydrocarbon filling retards or inhibits cementation [30−32], particularly carbonate cementation. Statistics show that the contents of carbonate cements demonstrate an obvious reducing trend with the increasing of oil-bearing grade (Table 2). Meanwhile,

Table 2 Average contents of carbonate cements in different oil-bearing grade reservoirs

Oil-bearing grade	w_B/%					Number of sample
	Total carbonate cement	Calcite	Ferrocalcite	Dolomite	Ankerite	
Oil free	13.92	6.85	1.5	4.25	1.32	30
Fluorescence	12.13	6.96	2.2	2.5	0.47	23
Oil trace	11.2	6.55	0.9	3.1	0.65	20
Oil stain	8.39	4.53	1.2	2.06	0.6	58
Oil soaked	6.28	3.6	0.3	1.88	0.5	68
Oil saturated	3.5	2.5	0	0.8	0.2	10

carbonate cementation shows euhedral crystals growth in reservoirs with a high oil-bearing grade (Figs. 8(a) and (b)). It can be inferred that early hydrocarbon filling predates carbonate cementation and inhibits carbonate cementation obviously. In the contrast, extensive carbonate cementation has been identified with high contents in poor or no oil-bearing reservoirs (Fig. 8(c)). On the other hand, overpressures caused by early hydrocarbon filling can retard compaction and protect primary pores in the deep strata (Fig. 4(d), Figs. 8(a) and (b)).

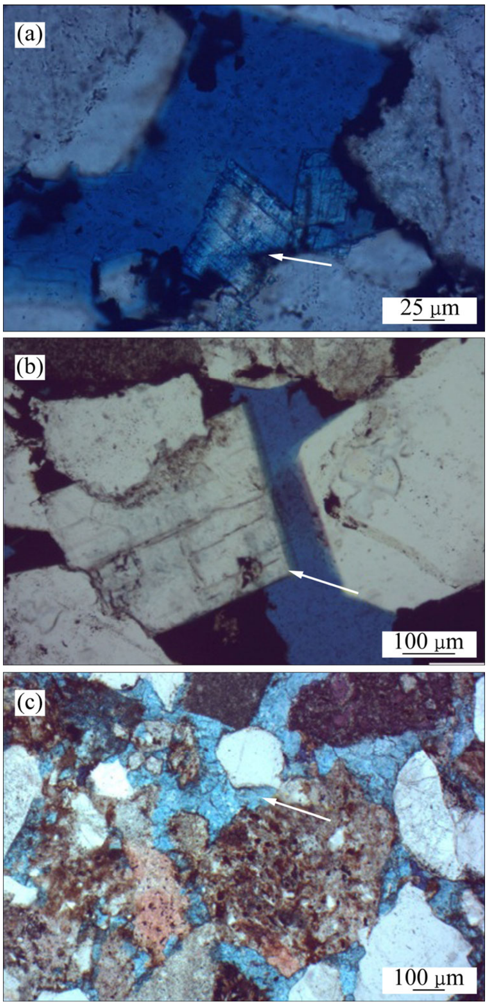

Fig. 8 Characteristics of carbonate cementation in different oil-bearing grade reservoirs: (a) Well Yi173, 4116 m, ankerite occurring as euhedral crystals in oil saturated reservoir; (b) Well Yi173, 4115.2 m, dolomite occurring as euhedral crystals in oil soaked reservoir; (c) Well Yi284, 3804 m, pore-filling blocky ankerite in oil free reservoir

4.3 Dissolution by early organic acids

There are mainly two sets of source rocks in Es4s and Es3x with a maximum thickness of 600 m in the northern steep slope zone of the Bonan sag [7, 33−34]. The source rocks are of high quality, which mainly consist of oil shales and dark mudstones in semi-deep and deep lacustrine [7], with kerogen types I and II in the majority.

Previous studies show that formation of abundant secondary porosity requires an interaction between sandstones and acidic fluids [35−36]. These fluids could have been meteoric origin or probably carboxylic and carbonic in composition derived from the diagenesis of buried organic matters in the source rocks prior to oil generation [37−38]. Generally, $\delta^{18}O$ values of meteoric water range from −12‰ to 0‰(SMOW) [39−40]. According to calcite−water [41] and dolomite-water fractionation equation [42], $\delta^{18}O$ values of lake water could be calculated and range from −3.94‰ to 9.57‰ with an average of 2.52‰ (SMOW) [43] (Table 3), when calcite and dolomite were precipitated. Therefore, it is indicated that meteoric water has little impact on diagenesis of Es4 reservoirs and most of the secondary pores in deep reservoirs are generated due to dissolution by organic acids.

SURDAM et al [37], based on quantities of experimental work, argued that the temperatures for the maximum concentrations of short-chain carboxylic acids(the peak of oxygen-containing groups released by kerogen) are 75−90 °C, and the optimal temperature for organic acids preservation is 80−120 °C [37]. Besides, geothermal gradient was high with a value of 4.6 °C/100 m in the depositional period of Es4s in the northern steep slope zone of the Bonan sag [44], and thus thermal maturation of the source rocks in the study area could be accelerated.

Table 3 $\delta^{18}O$ data of carbonate cements in Es4 from Bonan sag ($\delta^{18}O$ data quoted from [43])

Well	Depth/m	Strata	Carbonate cement	$\delta^{18}O$-PDB/‰	$\delta^{18}O$-SMOW/‰	$\delta^{18}O$-SMOW(H_2O)/‰
Yi17	3430.9	Es4	Ferrocalcite	−7.96	22.70	8.06
Yi17	3515.7	Es4	Ferrocalcite	−9.21	21.42	6.77
Yi160	3579.49	Es4	Ferrocalcite	−17.05	13.33	−1.32
Yi160	3582.2	Es4	Calcite	−11.72	18.82	4.18
Yi160	3594.4	Es4	Dolomite	−16.76	13.63	−1.02
Yi160	3595.5	Es4	Calcite	−16.22	14.19	−0.46
Yi160	3598.47	Es4	Calcite	−10.45	20.14	5.49
Yi160	3607	Es4	Calcite	−8.79	21.85	7.20
Yi160	3610	Es4	Calcite	−14.88	15.57	0.93
Yi160	3612.12	Es4	Ankerite	−15.58	14.85	0.20
Yi160	3678.69	Es4	Calcite	−8.88	21.76	7.11
Yi160	3679.29	Es4	Calcite	−17.76	12.60	−2.04
Yi160	3680.09	Es4	Calcite	−14.26	16.21	1.56
Yi160	3682	Es4	Calcite	−13.55	16.94	2.29
Yi170	3811.87	Es4	Ankerite	−18.69	11.64	−3.01
Yi170	3825	Es4	Ankerite	−14.47	15.99	1.34
Boshen5	4760	Es4	Ferrocalcite	−11.04	19.53	4.88
Boshen5	5138	Es4	Ferrocalcite	−6.49	24.22	9.57
Boshen4	5447	Es4	Calcite	−19.60	10.71	−3.94

Well Yi283 is a typical well which lies in the northern steep slope zone of the Bonan sag (Fig. 1). The generation and preservation of organic acids could be determined by the thermal evolution of the source rocks in Es4s and Es3x of Well 283 (Fig. 9). Formation temperature of the base of Es4s reached 75 °C about 42.5 Ma ago. With the burial depth increasing, formation temperature of the top and the base increased to 100 °C and 120 °C approximately 30 Ma ago. In consequence, organic matter began to mature and produce abundant organic acids during this period [37]. Under acidic conditions dominated by early organic acids with a temperature of 100−120 °C, organic acids could flow into reservoirs easily. As a result, vast of the secondary porosity was created by the dissolution of feldspars, rock fragments and other unstable grains (Figs. 4(a) and (b)). A certain quantity of SiO_2 was formed in the process of feldspars dissolution and it would be precipitated as quartz overgrowths in suitable conditions [45]. Under thin section observation, straight, syntaxial, euhedral and well-developed quartz overgrowths are common around detrital quartz grains in hydrocarbon filling reservoirs. The width of overgrowths ranges from 25.4 μm to 94.5 μm with an average of 57.6 μm. The average T_h for salt-water fluid inclusions in quartz overgrowths is 101.3 °C (Table 4), and the formation time can be calculated as about 40 Ma ago in conjunction with the burial history of Well Boshen 5. It is also consistent with the time when organic acids are released from source rocks.

Feldspar dissolution pores were filled with oil, suggesting that early dissolution predated early hydrocarbon filling (Fig. 4(a)). Therefore, feldspars dissolution as well as quartz overgrowths would not be hampered by early hydrocarbon filling, and there was enough space for quartz overgrowths to develop euhedral crystals. Quartz overgrowths are an important factor that can cause reservoir quality worse in many deep hydrocarbon reservoirs [46]. In fact, quartz cements, specifically syntaxial quartz overgrowths, are a major cause of porosity-loss in many petroleum reservoirs in both moderately to deeply buried reservoirs [47].

As mentioned above, early overpressures reached a maximum about 32.5 Ma ago, and at that time the source rocks (the whole Es4s and most of Es3x) were within optimal temperature range for organic acids preservation (Fig. 9). A large number of micro-fractures were produced by early overpressures and they would be important migration pathways for organic acid fluids. Furthermore, early overpressures had retarded organic matter maturity [48−49], and enabled the organic acids which had flowed into reservoirs already to stay in an acid environment over a long period, and thus helped to enhance reservoir dissolution.

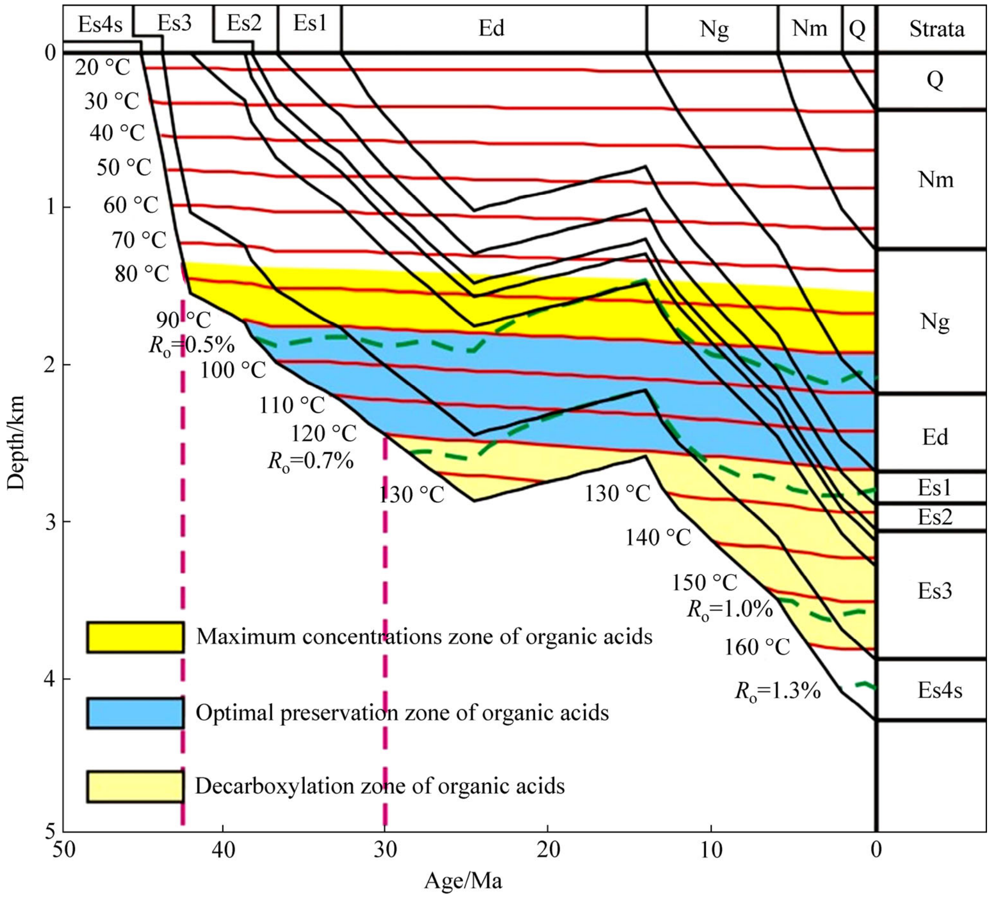

Fig. 9 Burial history of well Yi283 in northern steep slope zone of Bonan sag (R_o is the vitrinite reflectance)

Table 4 Data of fluid inclusions of Es4s reservoirs

Well	Depth/km	Strara	Lithofacies	Host mineral	Type	Size/μm	T_h/°C	Mean T_h/°C
Boshen 5	5136	Es4s	Pebbly sandstone	Quartz overgrowth	Salt-water	4	100.8	
Boshen 5	5136	Es4s	Pebbly sandstone	Quartz overgrowth	Salt-water	4.5	101.2	
Boshen 5	5136	Es4s	Pebbly sandstone	Quartz overgrowth	Salt-water	5.1	99.1	101.3
Boshen 5	5136	Es4s	Pebbly sandstone	Quartz overgrowth	Salt-water	6.2	103	
Boshen 5	5136	Es4s	Pebbly sandstone	Quartz overgrowth	Salt-water	6.5	102.4	

5 Reservoirs evaluation and sweet spots prediction

5.1 Reservoirs evaluation

A comprehensive evaluation which includes parameters of macroscopic physical property and microcosmic pore-throat texture, combined with thin section observation and oil testing results, was adopted to assess reservoir quality. As a result, the sandy conglomerate reservoirs are divided into four types in Es4s in the northern steep slope zone of the Bonan sag (Table 5).

Porosities of type I reservoirs range from 9.6% to 17.6% with an average of 14.8% and its permeabilities range from 5.44 mD to 135.65 mD with an average of 43.98 mD, which indicate that type I reservoirs have the best physical properties. p_d as a mercury-penetration parameter ranges from 0.01 MPa to 0.5 MPa with an average of 0.23 MPa. pc_{50} as the other mercury-penetration parameter ranges from 0.3 MPa to 8 MPa with an average of 2.61 MPa. Reservoir space is well developed and composed of secondary pores predominantly as well as minor primary pores. Pore-throat textures are characterized by middle pores and thin throats system with a better connectivity between them. Type I reservoirs are high-quality ones with a daily oil production more than 10 t as evidenced by oil testing results. For instance, brown sandy conglomerate reservoirs in the braided channel of middle fan in Well Yi 282 at the burial depth of 3460.35−3461.90 m have a daily oil production of 13.9 t.

Table 5 Reservoir classification in deep strata of Es4s in northern steep slope zone of Bonan sag (p_d represents displacement pressure, p_{c50} represents corresponding capillary pressure at value of 50% Hg saturation in capillary pressure curves)

Item			Type I	Type II	Type III	Type IV
Capillary pressure curve			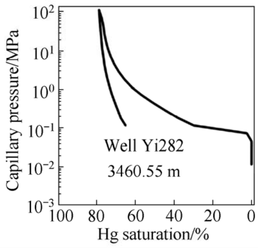	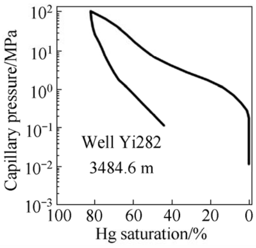	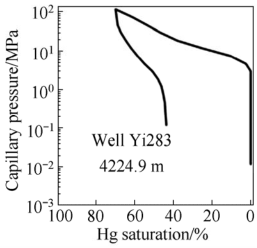	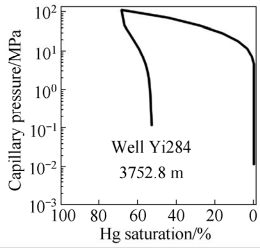
Physical property	Prosity/%	Average	14.8	10.8	6.4	3.6
		Min	9.60	6.4	3.1	1.3
		Max	17.6	14.8	9.5	5.5
	Perme-ability/mD	Average	43.98	9.25	0.89	0.210
		Min	5.44	1.47	0.15	0.021
		Max	135.65	29.31	3.12	0.397
Mercury penetration parameter	p_d/MPa	Average	0.23	0.74	2.13	4.82
		Min	0.01	0.25	0.80	2.45
		Max	0.50	2.01	4.25	10.0
	p_{c50}/MPa	Average	2.61	10.21	35.55	60.82
		Min	0.30	0.53	2.02	8.35
		Max	8.00	23.55	75.45	95.73
Thin section characteristics			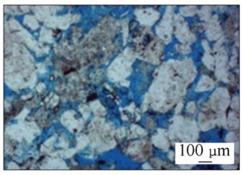 Well Yi282, 3460.55 m (−) Secondary pores predominatly and minor primary pores with a good connectivity between pores and throats	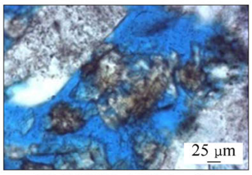 Well Yi282, 3684.6 m (−) Secondary pores pores well developed with a relatively good connectivity between pores and throats	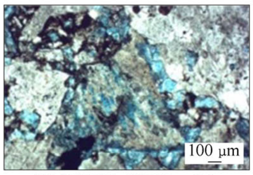 Well Yi283, 4227.7 m (−) Minor secondary pores developed locally with a relatively poor connectivity between pores and throats	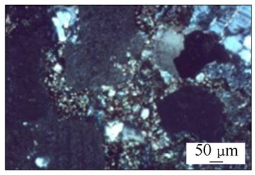 Well Yi285, 4179.55 m (+) No pores identified with a extremely poor connectivity between pores and throats

Porosities of type II reservoirs range from 6.4% to 17.6% with an average of 10.3% and its permeabilities range from 1.47 mD to 29.31 mD with an average of 9.25 mD, which indicate that type II reservoirs have relatively good physical properties. p_d ranges from 0.25 MPa to 2.01 MPa with an average of 0.74 MPa. p_{c50} ranges from 0.53 MPa to 23.55 MPa with an average of 10.21 MPa. Reservoir space mainly consists of secondary pores. Pore-throat textures are characterized by small pores and thin throats system with a relative good connectivity between them. Type II reservoirs are relatively high quality ones with a daily oil production from 5 t to 10 t as evidenced by oil testing results. For instance, oil-bearing fine sandstone reservoirs in the braided channel of middle fan in Well Yi 173 at burial depths of 4108.35−4124.5 m have a daily oil production of 6.51 t.

Porosities of type III reservoirs range from 3.1% to 9.5% with an average of 6.4% and its permeabilities range from 0.15 mD to 3.12 mD with an average of 0.89 mD, which indicate that type III reservoirs have relatively poor physical properties. p_d ranges from 0.8 MPa to 4.25 MPa with an average of 2.13 MPa. p_{c50} ranges from 2.02 MPa to 75.45 MPa with an average of 35.55 MPa. Reservoir space is locally developed along with a small amount of secondary pores. Pore-throat textures are characterized by small pores and micro-throats system with a relatively poor connectivity between them. Type III reservoirs, as the transitional ones in the study area, are of relatively poor quality with a daily oil production less than 5 t as evidenced by oil testing results. For instance, gray sandy conglomerate reservoirs in the braided channe of middle fan in Well Yi 283 at depths of 3957−3962 m are low oil yield with a daily oil production of 2.35 t.

Porosities of type IV reservoirs range from 1.3% to 5.5% with an average of 3.6% and its permeabilities range from 0.021 mD to 0.397 mD with an average of 0.21 mD, which indicate that type IV reservoirs have the worst physical properties. p_d ranges from 2.45 MPa to 10 MPa with an average of 4.82 MPa. p_{c50} ranges from 8.35 MPa to 95.73 MPa with an average of 60.82 MPa.

Almost no reservoir space could be identified in this type of reservoirs. Pore-throat textures are characterized by micro-pores and micro-throats system with an extremely worse connectivity between them. Type IV reservoirs are of extremely poor quality dominated by dry layers as evidenced by oil testing results. For instance, matrix-supported conglomerate reservoirs in the inner fan in Well Yi 110 at depths of 3521−3537 m are still dry layers after hydraulic fracturing measures.

5.2 Sweet spots prediction

Nearshore subaqueous fans are composed of sandy conglomerate bodies with a complex superposition of multi-cycle, normal graded sequences that are controlled by episodic fault activities and climate conditions, and the profile of sandy conglomerate bodies is as below(from bottom to top vertically): mud-rock flows deposition, paroxysmal flood deposition, normal stream deposition during flood intervals and suspended lacustrine deposition. Generally, sandy conglomerate bodies are characterized with a positive cycle deposition, although there may be lack of some sediments in different sub/micro-facies of nearshore subaqueous fan [50]. The sedimentary characteristics in different sub/micro-facies of nearshore subaqueous fan control different diagenetic responses, and meanwhile determine different evolution of reservoir physical properties. The distance to boundary faults in the source direction for reservoirs in different sub/micro-facies is calculated, and therefore, the distribution of different types of reservoirs is plotted (Fig. 10).

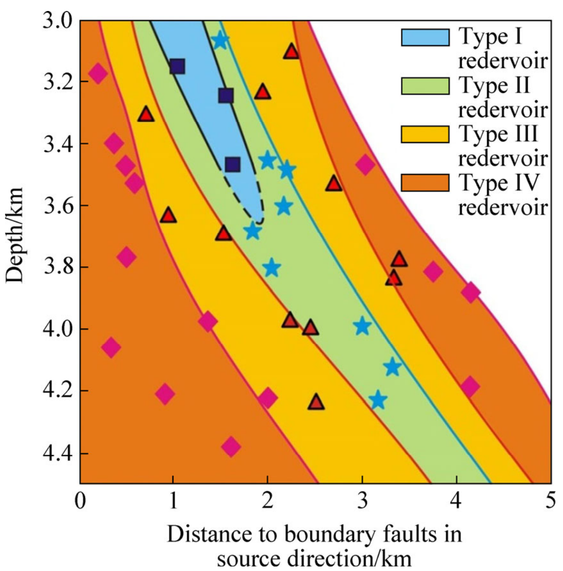

Fig. 10 Relationship between distribution of reservoir types and distance to boundary faults in source direction

Lithologies of the inner fan are mainly distinguished by poor sorted, coarse grained, matrix supported conglomerate with high calcareous matrix contents. The inner fan had a poor initial physical property and mainly experienced strong compaction and calcareous matrix recrystallization. Abundant primary pores were destroyed due to early rapid compaction. As a result, organic acids were difficult to flow into the inner fan because of the far distance from source rocks, and meanwhile, dissolved products were difficult to migrate out. The inner fan close to boundary faults was difficult to form effective protection by early overpressures because of the early faults activities. With an increase of burial depth, physical properties of the inner fan drastically decreased due to calcareous matrix recrystallization and would become sealed layers in deep strata. Distribution for these type IV reservoirs extends with the burial depth (Fig. 10).

Lithologies of the braided channel microfacies in the middle fan are characterized by massive pebbly sandstones and medium-coarse sandstones with moderately-well sorted, low matrix contents and high textural maturity. The braided channel reservoirs had a better initial physical property and stronger ability to resist compaction as well. Although a portion of primary pores was lost during early rapid compaction, abundant organic acids generated by organic matters maturity still flowed into the braided channel reservoirs and as a result, large amounts of the secondary porosities were created by the dissolution of feldspars, rock fragments and other unstable grains. Early overpressures reached the first peak about 32.5 Ma ago due to disequilibrium compaction during the early rapid deposition. On one hand, early overpressure could hamper early compaction and protect primary pores. On the other hand, a series of micro-fractures were generated from early overpressures, which would be important migration pathways for hydrocarbon and organic acids. Furthermore, early overpressures had retarded maturation of organic matters, and organic acids which had flowed into reservoirs already could keep in acid environment for a long time. This process would contribute significantly to reinforcing the dissolution and enhance the reservoir quality. With the continuing subsidence of the strata, early hydrocarbon filling took place approximately from 28.8 Ma to 24.6 Ma ago, and in this process reservoirs with better physical properties in the braided channel were filled with large amounts of hydrocarbon preferentially, which results in reservoirs having high oil saturation. The reservoirs with high oil saturation could effectively inhibit later carbonate cementation, and had a good protection against the reduction of physical properties. Paleopressures were reducing rapidly as a result of regional tectonic uplift and reached the minimum about 24.6 Ma ago. Afterwards, the formation temperature rose quickly with the strata subsidence again, and source rocks of Es4s and Es3x entered into thermal mature stage. Therefore, the paleopressures increased once again due to the hydrocarbon generation and reached the second peak when generally source rocks in Es4s and Es3x were still in optimal temperature ranges for organic acids preservation. The early sealed micro-fractures were opened up again as a result of the hydrocarbon generation in the later period, which would be vital migration pathways for hydrocarbon and organic acid fluids. Physical properties and oil-bearing grade of the reservoirs were improved effectively by the existence of micro-fractures. Reservoir types of the braided channel microfacies mainly are types I, II and III. The difference of reservoir types is caused by the difference of initial sedimentary characteristics. The better reservoir types are of well-sorted, stronger ability to resist compaction, better dissolution by early organic acids, larger amounts of early hydrocarbon filling, more intensive inhibition of the later carbonate cementation. Distributions of type I and type II reservoirs are narrowed with the increasing burial depth, that is, the scope of “sweet spots” zones is reduced (Fig. 10). Type III reservoirs, as discussed above, are the transitional type of reservoirs in the study area, of which the distribution narrowes first and then extends

Lithologies of the interdistributary in middle fan and thin sand layers in outer fan are characterized by fine-grained sediments (fine-grained sandstones and pelitic siltstones) in majority and minor pebbled sandstones. Sandstones in the interdistributary microfacies are poor sorted with high contents of matrix due to the poor initial hydrodynamic conditions. Therefore, reservoirs in the interdistributary microfacies had poor physical properties after early rapid compaction. In the process of early hydrocarbon filling, hydrocarbon would preferentially fill into the braided channel that lay in high structural positions and had better physical properties, rather than thin sandbodies in outer fan that lay in a relatively low structural position. In the contrast, reservoirs in both interdistributary microfacies and outer fan were charged by limit hydrocarbon with low oil saturation. Previous studies showed that there was a close relationship between oil saturation and prohibitive effect on reservoir diagenesis by hydrocarbon. Only when reservoir pores were completely or mostly occupied by hydrocarbon, resulting in pore water in a discontinuous and isolated state, could diagenesis be inhibited from carrying on. Otherwise, as long as pore water could flow freely, and reservoir diagenesis would not cease [51]. Therefore, the hydrocarbon injected into the reservoirs both in interdistributary microfacies and outer fan had a limit inhibition to the later diagenesis, and thus the reservoirs would be extensively cemented by carbonate with an extremely poor physical property, which was type IV (Fig. 10).

Through comprehensive analysis, it is concluded that, firstly, sedimentation is the fundamental of forming high quality reservoirs in the deep strata. Only reservoirs with better initial sorting in the braided channel can preserve abundant primary pores, resulting in extensive dissolutions by organic acid flowing into reservoirs largely. These reservoirs could be protected effectively by early overpressures and hydrocarbon filling, and become present zones of “sweet spots”. Secondly, diagenesis is a key factor that controls the effectiveness of reservoirs in the deep. Strong compaction and calcareous matrix recrystallization along with weak dissolution took place in the inner fan and as a result, its physical property is poor and effective reservoirs can hardly be developed in the deep. By comparison, extensive dissolutions by organic acid are commonly observed in the braided channel reservoirs and moreover, carbonate cementation is fiercely inhibited by subsequently early hydrocarbon filling, resulting in plenty of effective reservoirs developed in the deep. Pervasive carbonate cementation is developed both in outer fan and the interdistributary of middle fan because of limited or no hydrocarbon filling, and therefore physical properties of these reservoirs are extremely poor and hardly any effective reservoirs are developed in the deep. Thirdly, overpressures are protective conditions for high quality reservoirs in the deep. They can retard formation compaction effectively and protect reservoir pores against destruction in the deep. However, only when reservoirs have good conditions for original deposition could they be effectively conserved by the overpressures and form as high quality ones in the deep. In the contrast, reservoirs with poor initial sedimentary conditions that can be destroyed seriously by the later diagenesis, can hardly turn into high quality ones even if the overpressures existed.

Oil testing data indicate that a majority of oil layers as well as minor water layers can be observed below the burial depth of 3250 m in the nearshore subaqueous fans of Es4s in the northern steep slope zone of the Bonan sag; while at the burial depth less than 3250 m, oil layers become less and water layers increase from deep to shallow strata (Fig. 11). The reason for this phenomenon is that the lateral sealing capacity of inner fan is poor in relatively shallow strata (above 3250 m) and under the circumstance of lack of structural traps, it is difficult to form effective hydrocarbon accumulation (or form small scales of lithologic hydrocarbon reservoirs) even though effective reservoirs are developed. In the contrast, large scales of lithologic hydrocarbon reservoirs can be formed due to the inner fan with a strong lateral sealing capacity despite of the lack of structural traps in the deep strata (below 3250 m). Therefore, the distribution of “sweet spots” in the deep strata, on one hand, is controlled by the distribution of high quality reservoirs, and on the other hand, will depend on the sealing capacity of the inner fan which is laterally connected with the braided channel reservoirs. Only when the inner fan has a definite sealing capacity can it effectively seal hydrocarbons accumulated in the braided channel reservoirs.

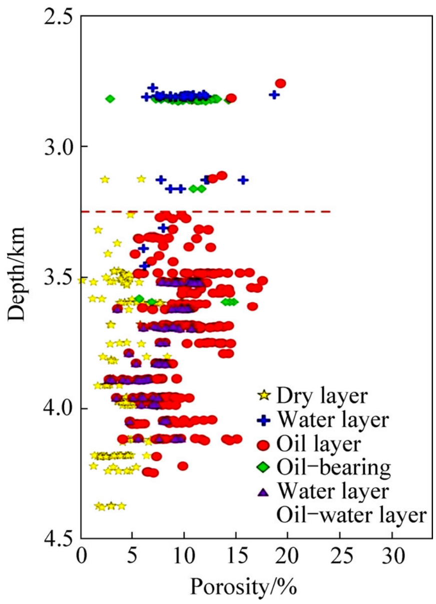

Fig. 11 Relationship between depth, porosity and oiliness of nearshore subaqueous fan of Es4s in northern steep slope zone of Bonan sag (Oil testing results combined with measured properties and logging interpretation properties for a total of 282 samples from 25 wells)

6 Conclusions

1) The deep reservoirs of Es4s in the northern steep slope zone of the Bonan sag have poor physical properties and mainly develop extra-low porosity, extra-low and ultra-low permeability reservoirs. The reservoir space mainly includes secondary pores and overpressure fractures.

2) Early overpressure, early hydrocarbon filling, dissolution by early organic acids are the major formation mechanisms of high quality reservoirs in the deep strata. Firstly, porosity, which would be lost by progressive compaction, is held by early overpressures, resulting in anomalously porous reservoirs in the deep strata; Secondly, early hydrocarbon filling retard or inhibit cementation effectively and overpressures caused by early hydrocarbon filling can retard compaction and protect primary pores in the deep strata; Thirdly, early organic acids dissolution, particularly feldspar dissolution, could greatly enhance reservoir quality and raise reservoir oiliness.

3) The sandy conglomerate reservoirs are divided into four types in the deep strata of Es4s in the northern steep slope zone of the Bonan sag. Sedimentary characteristics in different sub/micro-facies of nearshore subaqueous fan control different diagenetic response, and finally determine different evolution of reservoir physical properties. The conglomerate in inner fan mainly experiences strong compaction and calcareous matrix recrystallization. The reservoirs with poor physical properties in inner fan mainly develop type IV reservoirs and the distribution of them extends with the burial depth. Due to reconstructed by early overpressure, early hydrocarbon filling and dissolution by early organic acids, braided channel reservoirs in the middle fan develop a great quantity of reservoir spaces with type I, type II and type III reservoirs domanted. Distribution of type I and type II reservoirs are narrowed, that is, the scope of “sweet spots” zones is reduced and distribution of type III reservoirs decreases first and then extends with the burial depth. The reservoirs both in outer fan and in interdistributary of middle fan have extremely poor physical properties because of extensive carbonate cementation. The type of the reservoirs mainly is type IV.

4) Sedimentation is the fundamental of forming high quality reservoirs in the deep strata. Diagenesis is a key factor that controls the effectiveness of reservoirs. Overpressures are protective conditions for high quality reservoirs. The distribution of “sweet spots” in the deep strata, on one hand, is controlled by the distribution of high quality reservoirs, and on the other hand, will depend on the sealing capacity of the inner fan. Only when the inner fan has a definite sealing capacity, can it effectively seal hydrocarbons accumulated in the braided channel reservoirs.

References

[1] AJDUKIEWICZ J M, NICHOLSON P H, ESCH W L. Prediction of deep reservoir quality using early diagenetic process models in the Jurassic Norphlet Formation, Gulf of Mexico [J]. AAPG Bulletin, 2010, 94(8): 1189−1227.

[2] MIDTBØ R E, RYKKJE J M, RAMM M. Deep burial diagenesis and reservoir quality along the eastern flank of the Viking Graben. Evidence for illitization and quartz cementation after hydrocarbon emplacement [J]. Clay Minerals, 2000, 35: 227−237.

[3] WANG Yan-zhong, CAO Ying-chang, LI Yong-xin, WANG Shu-ping, XI Ke-lai. Controlling factors on the Paleogene deep effective reservoirs in the Bonan sag [J]. Natural Gas Geoscience, 2012, 23(6): 996−1003. (in Chinese)

[4] BLOCH S, LANDER R H, BONNELL L. Anomalously high porosity and permeability in deeply buried sandstone reservoirs: Origin and predictability [J]. AAPG Bulletin, 2002, 86(2): 301−328.

[5] YANG You-xing, JIN Zhen-kui, LU Yan-xia, DIAO Li-ying, WANG Pu, LIU Chun-hui. Characteristics and formation of high quality reservoirs in sediment gravity flows of Gangzhong area, Huanghua depression [J]. Journal of Central South University, 2014, 21(2): 745−752.

[6] ZHANG Jin-liang, LI De-yong, JIANG Zhi-qiang. Diagenesis and reservoir quality of the fourth member sandstones of Shahejie

formation in Huimin depression, eastern China [J]. Journal of Central South University, 2010, 17: 169−179.

[7] XU Xing-you, XU Guo-sheng, TAI Rui-shen. Study on hydrocarbon migration and accumulation of Member 4 of Shahejie Formation in Bonan sag, Zhanhua depression, China [J]. Journal of Chengdu University of Technology: Science & Technology Edition, 2008, 35(2): 113−120. (in Chinese)

[8] GUO Rui-chao, LI Yan-jun, WANG Ting-dong, SONG Guo-qi, LI Wen-tao, YIN Chang-he, LIU Chen. Oil−gas source and accumulation characteristics of paleogene in Bonan sub-sag in Shengli Oil Field [J]. Xinjiang Petroleum Geology, 2009, 30(6): 674−676. (in Chinese)

[9] ZHANG Zhi-huan, ZENG Yan-tao, ZHANG Xue-jun, YUAN Dong-shan, XU Xing-you. The geochemistry characteristics and accumulation-history of crude oil in the Bonan sub-sag of the Zhanhua sag, the BohaiwanBasin [J]. Petroleum Geology & Experiment, 2006, 28(1): 54−58. (in Chinese)

[10] LIU Hua, JIANG Yu-lu, GU Guo-cui, LIU Ya-li, LU Hao. Pressure characteristics and formation mechanisms of Paleogene in Bonan sag, Zhanhua depression [J]. Journal of China University of Petroleum, 2013, 37(4): 46−51. (in Chinese)

[11] ZAN Ling, ZHANG Zhi-huan, WANG Shun-hua, FENG Wu-jun, ZHANG Li-sheng, XING Hui. Diagenesis of sandy conglomerate reservoir in northern steep slope of Bonansubsag [J]. Natural Gas Geoscience, 2011, 22(2): 299−305. (in Chinese)

[12] ZHONG Wei-ping, CAO Ying-chang, WANG Yan-zhong, LIU Hui. The types and distribution of the sand bodies in Sha4 member in Bonan Depression [J]. Petroleum Geology and Recovery Efficiency, 2010, 17(1): 48−51. (in Chinese)

[13] FOLK R L. Petrology of sedimentary rocks [M]. Texas: Hemphill Press, 1968: 107−108.

[14] CAO Ying-chang. Quantitative prediction for effectiveness of low permeability reservoirs in Jiyang depression [R]. Qingdao: China University of Petroleum, 2013. (in Chinese)

[15] KOUKETSU Y, NISHIYAMA T, IKEDA T, ENAMI M. Evaluation of residual pressure in an inclusion–host system using negative frequency shift of quartz Raman spectra [J]. American Mineralogist, 2014, 99: 433−442.

[16] LI Chang-cun, HAN Xiu-li, ZOU Ji-xing. Study on fluid inclusion of Luanmuchang gold deposit [J]. Mineral Petrol, 1999, 19(1): 55−57. (in Chinese)

[17] ZHANG Y G, FRANTZ J D. Determination of the homogenization ternperature and densities of supercritical fluids in the system $NaCl-KC1-CaCl_2-H_2O$ using synthetic fluid inclusions [J]. Chemical Geology, 1987, 64: 335−350.

[18] CHEN Yong, ZHOU Yao-qi, NI Pei. A new method for measurement of internal pressure of inclusions: CO_2-Raman spectrometry [J]. Rock and Mineral Analysis, 2006, 25(3): 211−214. (in Chinese)

[19] OSBORNE M J, SWARBRICK R E. Mechanisms for generating overpressure in sedimentary basins: A reevaluation [J]. AAPG Bulletin, 1997, 81(6): 1023−1041.

[20] RAMDHAN A M, GOULTY N R. Overpressure and mudrock compaction in the Lower Kutai Basin, Indonesia: A radical reappraisal [J]. AAPG Bulletin, 2011, 95(10): 1725−1744.

[21] TAYLOR T R, GILES M R, HATHON L A, DIGGS T N, BRAUNSDORF N R, BIRBIGLLA G V, KITTRIDGE M G, MACAULAY C L, ESPEJO I S. Sandstone diagenesis and reservoir quality prediction: Models, myths, and reality [J]. AAPG Bulletin, 2010, 94(8): 1093−1132.

[22] PU Xiu-gang, ZHOU Li-hong, WANG Wen-ge, HAN Wen-zhong, XIAO Dun-qing, LIU Hai-tao, CHEN Chang-wei, ZHANG Wei, YUAN Xuan-jun, LU Yi, LIU Sa. Medium-deep clastic reservoirs in the slope area of Qikou sag, Huanghua depression, Bohai Bay basin [J]. Petroleum Exploration and Development, 2013, 40(1): 36−48. (in Chinese)

[23] BLOCH S, LANDER R H, BONNELL L M. Anomalously high porosity and permeability in deeply buried sandstone reservoirs: Origin and predictability [J]. AAPG Bulletin, 2002, 86(2): 301−328.

[24] BECKER S P, EICHHUBL P, LAUBACH S E, REED R M, LANDER R H, BODNAR R J. A 48 m.y. history of fracture opening, temperature, and fluid pressure: cretaceous travis peak formation, East Texas basin [J]. Geological Society of America Bulletin, 2010, 122(7/8): 1081−1093.

[25] NGUYEN B T T, JONES S J, GOULTY N R, MIDDLETON A J, GRANT N, FERGUSON A, BOWEN L. The role of fluid pressure and diagenetic cements for porosity preservation in Triassic fluvial reservoirs of the central Graben, North Sea [J]. AAPG Bulletin, 2013, 97(8): 1273−1302.

[26] ZENG Lian-bo. Microfracturing in the Upper Triassic Sichuan Basin tight-gas sandstones: Tectonic, overpressure, and diagenetic origins [J]. AAPG Bulletin, 2010, 94(12): 1811−1825.

[27] HAO Fang. Kinetics of hydrocarbon generation and mechanisms of petroleum accumulation in overpressure basin [M]. Beijing: Science Press, 2005. (in Chinese)

[28] CAO Ying-chang, JIA Yan-cong, WANG Yan-zhong, MA Ben-ben. Diagenetic fluid evolution of reservoirs in Es4s in the north zone of the Bonan sag [J]. Geoscience, 2014, 28(1): 1−10. (in Chinese)

[29] CAO Ying-chang, MA Ben-ben, WANG Yan-zhong, LI Xue. Genetic mechanisms and classified evaluation of low permeability reservoirs of Es4s in the north zone of Bonan sag [J]. Natural Gas Geoscience, 2013, 24(5): 865−875.

[30] JIN Zhi-jun, CAO Jian, HU Wen-xuan, ZHANG Yi-jie, YAO Su-ping, WANG Xu-long, ZHANG Yue-qian, TANG Yong, SHI Xin-pu. Episodic petroleum fluid migration in fault zones of the northwestern Junggar Basin (northwest China): Evidence from hydrocarbon-bearing zoned calcite cement [J]. AAPG Bulletin, 2008, 92(9): 1225−1243.

[31] MOLENAAR N, CYZIENE J, SLIAUPA S, CRAVEN J. Lack of inhibiting effect of oil emplacement on quartz cementation: Evidence from Cambrian reservoir sandstones, Paleozoic Baltic Basin [J]. Geological Society of America Bulletin, 2008, 120(9/10): 1280−1295.

[32] AASE N E, WALDERHAUG O. The effect of hydrocarbons on quartz cementation: Diagenesis in the Upper Jurassic sandstones of the Miller Field, North Sea, revisited [J]. Petroleum Geoscience, 2005, 11: 215−223.

[33] GONG Xiu-mei, JIN Zhi-jun, ZENG Jian-hui, QIU Nan-sheng. Resrvoiring characteristics and main controlling factors for deep hydrocarbon accumulations in Bonan sag in Jiyang depression [J]. Oil & Gas Geology, 2005, 26(4): 473−479. (in Chinese)

[34] WU Fu-qiang, LI Hou-shu, HU Xue, LIU Jia-duo, SUN Xi-wen. An approach to the composite petroleum systems of Es41 in Bonan sag, Shengli oil province [J]. Petroleum Exploration and Development, 2002, 29(3): 29−31. (in Chinese)

[35] MILLIKEN K L. Petrography and composition of authigenic feldspars, Oligocene Frio Formation, South Texas [J]. Journal of Sedimentary Petrology, 1989, 59: 361−374.

[36] WILKINSON M, MILLIKEN K L, HASZELDINE R S. Systematic destruction of K-feldspars in deeply buried rift and passive margin sandstones [J]. Journal of the Geological Society, 2001, 158: 675−683.

[37] SURDAM R C, BOESE S W, CROSSEY G J. The chemistry of secondary porosity [J]. AAPG Memoir, 1984, 37: 127−151.

[38] SURDAM R C, CROSSEY L J, HAGEN E S. Organic-inorganic interactions and sandstone diagenesis [J]. AAPG Bulletin, 1989, 73: 1−23.

[39] BECHTEL A, SAVIN S M, HOERNES S. Oxygen and hydrogen isotopic composition of clay minerals of the Bahloul Formation in

the region of the Bou Grine zine-lead ore deposit (Tunisia): Evidence for fluid-rock interaction in the vicinity of salt dome cap rock [J]. Chemical Geology, 1999, 156: 191−207.

[40] LAW E W, BURROWS S M, ARONSON J L, SAUIN S M. A petrologic, geochronologic, and oxygen isotopic study of the diagenesis of the Muddy Sandstone, east flank of the Powder River Basin [C]// 27th Annual Meeting, Program and Abstracts, Clay Minerals Society. 1990: 110.

[41] O'NEIL J R, CLAYTON R N, MAYEDA T K. Oxygen isotope fractionation in divalent metal carbonates [J]. The Journal of Chemical Physics, 1969, 51(12): 5547−5558.

[42] MATTHEWS A, KATZ A. Oxygen isotope fractionation during the dolomitization of calcium carbonate [J]. Geochimica et Cosmochimica Acta, 1977, 41: 1431−1438.

[43] WU Fu-qiang, XIAN Xue-fu, LI Hou-shu, LIU Jia-duo. Deep reservoir forming mechanism in the upper part of the fourth member of Shahejie Formation in Bonan subsag of Shengli Oil Field [J]. Acta Petrolei Sinica, 2003, 24(1): 44−47. (in Chinese)

[44] SU Xiang-guang, QIU Nan-sheng, LIU Zhong-quan, ZHANG Lin-ye, LI Zhao-ying. Tectonic-thermal evolution of Zhanhua sag [J]. Journal of Xi'an Shiyou University: Natural Science Edition, 2006, 21(3): 9−12. (in Chinese)

[45] RAHMAN M J, MCCANN, T. Diagenetic history of the Surma Group sandstones (Miocene) in the Surma Basin, Bangladesh [J]. Journal of Asian Earth Sciences, 2012, 45: 65−78.

[46] WORDEN R, MORAD S. Quartz cement in oil field sandstones: A review of the critical problems [J]. International Association of Sedimentolgists, 2000, 29: 1−20.

[47] WORDEN R, MORAD S. Clay minerals in sandstones: controls on formation, distribution and evolution [J]. International Association of Sedimentolgists, 2003, 34: 3−41.

[48] HAO Fang, ZOU Hua-yao, GONG Zai-sheng, WANG Shi-gang, ZENG Zhi-ping. Hierarchies of overpressure retardation of organic matter maturation: Case studies from petroleum basins in China [J]. AAPG Bulletin, 2007, 91(10): 1467−1498.

[49] MELLO U T, KARNER G D. Development of sediment overpressure and its effect on thermal maturation; application to the Gulf of Mexico basin [J]. AAPG Bulletin, 1996, 80(9): 1367−1396.

[50] GAO Yong-jin. Sedimentary cycle division and correlation of sand-conglomerate body: A case of upper Sha IV formation of Yanjia area, Jiyang depression [J]. Petroleum Geology and Recovery Efficiency, 2010, 17(6): 6−7. (in Chinese)

[51] WU Fu-qiang, NING Xing-xian. The controlling factors and processes for the formation of the secondary porosity of the deep-seated reservoir rocks in the Bonan depression, Shandong [J]. Sedimentary Geology and Tethyan Geology, 2004, 24(2): 76−82. (in Chinese)

(Edited by YANG Hua)